1995

Electric Field Mapping System With Nanosecond Temporal Rosolution

F. E. Peterkin
Old Dominion University

R. Block
Old Dominion University

K. H. Schoenbach
Old Dominion University

Original Publication Citation

Peterkin, F. E., Block, R., & Schoenbach, K. H. (1995). Electric field mapping system with nanosecond temporal resolution. *Review of Scientific Intruments, 66*(4), 2960-2966. doi:10.1063/1.1145583

Electric field mapping system with nanosecond temporal resolution

F. E. Peterkin, R. Block,[a] and K. H. Schoenbach
PERI Laboratory, Department of Electrical and Computer Engineering, Old Dominion University, Norfolk, Virginia 23529-0246

(Received 25 October 1994; accepted for publication 3 January 1995)

The electric field dependence of the absorption coefficient in semi-insulating GaAs at the absorption edge was measured in a high-voltage pulsed experiment. Pulse duration was kept below 50 ns in order to avoid thermal effects. A GaAs laser diode was used as a probe light source with wavelength varied from 902 to 911 nm. For fields up to 40 kV/cm the absorption coefficient increased from 3 to 17 cm^{-1} at 902 nm, with smaller absolute increases evident at the longer wavelengths. Calculation from theory was consistent with this behavior. The spatial variation of the electric field was also recorded with a CCD camera. This method was used as a diagnostic technique to study the field distribution during the switching cycle of a high-power photoconductive switch. The described system could be used as a simple electric field probe with temporal resolution of 100 ps, or as a field mapping system with spatial resolution approaching 1 μm. © *1995 American Institute of Physics.*

I. INTRODUCTION

Measurements of the electric field distribution in insulators and semiconductors under high electric stress allow us to determine the areas in the material where electrical breakdown is likely. Measures to improve the hold-off voltage can then be tested for their efficiency without the irreversible damage usually caused by electric breakdown. Optical methods are particularly attractive for field plotting because they are nonintrusive and permit measurement of transient fields with high temporal resolution. Two-dimensional imaging methods have been developed particularly for the study of semi-insulating gallium arsenide (GaAs) switches[1–4] but they can also be applied to other insulating and semi-insulating materials. The methods are either based on the measurements of the field-induced birefringence (electro-optic effect) or the field-induced change in the complex index of refraction (Franz–Keldysh effect) in the material of interest or in a material which is placed close to the sample which is to be studied.

In studies where the electro-optic effect was utilized, the temporal development of the electric field distribution in GaAs photoconductive switches was measured by placing a lithium tantalate ($LiTiO_3$) crystal on the surface of the switch.[1] The system was probed with linearly polarized light from a frequency-doubled Nd:YAG laser. The surface field of the GaAs switch caused local changes in the birefringence of the $LiTiO_3$ crystal, and consequently a rotation in the polarization plane of the probe laser light. The field-dependent polarization of the laser beam after passing through the birefringent crystal was recorded by means of a CID camera. The temporal resolution of this diagnostic technique is limited mainly by the probe laser pulse and can be extended to the picosecond range.

Instead of using an electro-optic crystal such as lithium tantalate, with its high linear electro-optic coefficient (a measure for the sensitivity of the device with respect to electric field at a given wavelength) of 30.3 pm/V, gallium arsenide itself can be utilized for electro-optic measurements. Although its electro-optic coefficient is only 1.6 pm/V, the high electric fields in GaAs switches allow the electro-optic recording of field structures. A cw Nd:YAG laser, operating at 1064 nm, has been used as the light source in an experiment performed at Boeing Defense and Space Group.[5] The temporal resolution was determined by the detector, a sampling streak tube with better than 100 ps resolution.

A second field-mapping method using electroabsorption has been investigated recently.[2–6] Electroabsorption is based on the shift in the edge of the absorption spectrum of an insulator or semiconductor (Franz–Keldysh effect) due to electric fields.[7] Illuminating a sample with light of wavelength corresponding to the band gap of the material makes it possible to obtain the spatial distribution of electric fields by recording the absorption pattern of the sample. The method works particularly well for direct semiconductors where the absorption coefficient at the band edge varies exponentially, changing by orders of magnitude over a narrow wavelength range. Small electric fields can induce large shifts in the absorption at a fixed wavelength.

Other workers have focused on the study of the electric field distribution in the prebreakdown phase. The propagation of slow velocity domains was observed by means of a CCD camera with a temporal resolution of ms and with continuous illumination of the sample.[5] More recent experiments have utilized a tunable Ti:sapphire laser with a pulse duration of 4 ns.[6] Research at Old Dominion University has aimed at developing a simple, less expensive method to record electric field distribution with nanosecond resolution. We have concentrated on GaAs as the detector material because of the host of commercially available, inexpensive laser diodes operating at around 900 nm. With tunable dye lasers or parametric oscillators, however, other direct semiconductors such as ZnSe can be used as probing materials.[8]

The GaAs laser diode we used was wavelength shifted through temperature control to vary strength of the absorption change. For the spatially resolved measurements, a CCD camera with digital image acquisition into an IBM PC served as the detector. The system allowed us to explore the break-

[a]Telekom, Fachhochschule Berlin, Germany.

 0034-6748/95/66(4)/2960/7/$6.00

down behavior of GaAs photoconductive switches.[2]

The disadvantage of this method compared to the electro-optic method is the rather difficult task of calibrating the system. In particular, thermal effects tend to shift the band edge in the same way as electroabsorption, and both can be significant in the presence of high fields. In this paper we describe our efforts to calibrate the absorption technique for GaAs as a probe material and to develop a simple quantitative technique for transient field distribution measurements.

II. ABSORPTION SHIFT MECHANISMS

First predicted by Franz[9] and Keldysh[10] independently, the Franz–Keldysh effect describes electric field-induced changes in the absorption spectrum of semiconductors and insulators due to photon-assisted tunneling across the band gap. The slope of the band edges in the presence of an electric field creates a finite probability that a drifting electron will tunnel into the forbidden gap. Less photon energy is then required to excite the electron into the conduction band or a deep trap. The net result is an increase in absorption probability and thus absorption coefficient. The greater the electric field, the more the absorption increases. The change is sufficiently large that GaAs has been investigated as an electroabsorption modulator in integrated optoelectronics applications.[11–13]

The Franz–Keldysh effect is only one mechanism which causes changes in the absorption spectrum of a semiconductor. Any physical process which affects the band gap of the semiconductor will shift the absorption edge. These include temperature, pressure, and magnetic field.[7] The shift in the band gap from these processes comes literally from the small changes in the interatomic spacing of the crystal. The absorption spectrum can also be altered by free-carrier absorption, which becomes comparable to field effects if the density is above about 10^{16} cm^{-3}.[14,15]

In the system which we have focused on, photoconductive GaAs switches, most of these other processes are not important. However, when an electric field is applied to a semiconductor we need to look at both temperature changes due to Joule heating and electric field as possible sources of change in the absorption measurements we make. A simple treatment of the Franz–Keldysh effect shows electroabsorption varies as[16]

$$\alpha \propto \exp\left(-\frac{4\sqrt{2m^*}(E_g-\hbar\omega)^{3/2}}{3eE\hbar}\right), \tag{1}$$

where α is the absorption coefficient, m^* is the electron effective mass, e is the electron charge, E_g is the band-gap energy, E is the electric field, and $\hbar\omega$ is the photon energy. Interpreting electroabsorption as a simple shift in the absorption edge to lower photon energies, a field of 50 kV/cm is required for an equivalent 10 meV shift. By comparison, the temperature dependence of the band gap in GaAs is such that a temperature change of 20 °C is also equivalent to a 10 meV shift. Thus we expect that thermal effects must be kept well below this level to have a meaningful result in this field range.

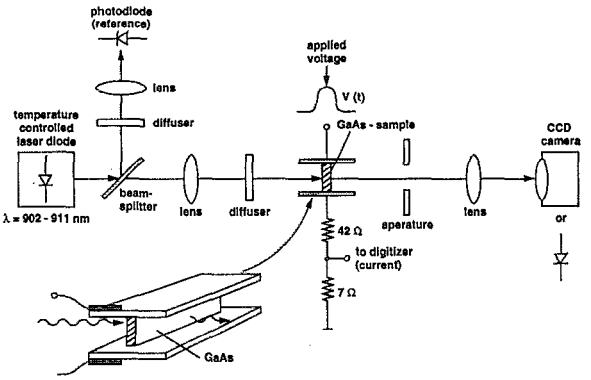

FIG. 1. Experimental setup for electroabsorption measurements.

Theoretical approaches to accurately describing the Franz–Keldysh effect include an electric field term in the Schrödinger equation and then solve to find the absorption coefficient from first principles.[17,18] These methods require extensive knowledge of fundamental material parameters which may be difficult or impossible to obtain. A more general approach to calculating the shift in the absorption spectrum was developed by Rees.[19] Using a perturbation method he calculated the change in transition probability resulting from field-induced momentum changes. The approach explicitly accounts for exciton effects and lattice scattering. The result is a relatively simple expression which expresses the shifted absorption spectrum as the convolution of the zero-field spectrum with an Airy function term which depends on the field:

$$\alpha(E,h\nu)=C\alpha(0,h\nu)*Ai(-C\cdot h\nu), \tag{2}$$

where

$$C=\left(\frac{32\pi^2 m^*}{h^2e^2E^2}\right)^{1/3}. \tag{3}$$

We use this method below to compare with the experimentally observed absorption changes.

III. EXPERIMENTAL SETUP

Figure 1 shows the schematic of our experimental setup. Semi-insulating GaAs with resistivity of 10^7 Ω cm was used as the material to be probed. The GaAs device under test (DUT) was cleaved from 4-in.-diam, 675-μm-thick double polished wafers. Care was taken to ensure the cleaved faces were as flat as possible. The DUT was placed between parallel plate brass electrodes with the cleaved faces pressed against the metal. Several devices of different size were tested, but the results we report here will be only for a device with 1.9 mm separation between the cleaved faces. The inset in Fig. 1 shows the orientation of the DUT was such that the optical probe illumination was directed through the polished faces of the GaAs and normal to the direction of the applied electric field.

Voltage pulses were generated using a charged coaxial transmission line and photoconductive switch as shown in

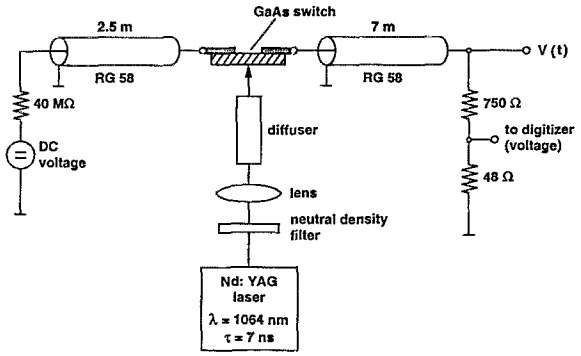

FIG. 2. Schematic of the high-voltage pulse generator.

Fig. 2. The 2.5-m-long, 50 Ω RG-8 cable was dc charged through a 40 MΩ resistor. The energy on the charged cable was switched into a 7 m section of RG-8 cable with a chrome-doped GaAs photoconductive switch triggered by an Nd:YAG laser. The termination of the 7 m cable was the output of the voltage generator and was monitored with a 775 Ω resistive voltage divider monitored by a 500 MHz Tektronix 7912 digitizing oscilloscope. The pulser was designed to be used with a load impedance much greater than the 50 Ω impedance of the cable. This meant the pulser output characteristic was a series of pulses with diminishing amplitude. Pulse width was determined by the 2.5 m cable and switch characteristics, while the spacing was determined by the transit time on the combined 2.5 and 7 m cable during switch turn on. For our purposes we were only interested in making measurements during the first pulse, when the amplitude (and applied electric field) was greatest. The pulse separation was unimportant, other than to ensure that we could probe after the pulse turned off to ensure that temperature effects were not important. Figure 3 shows a typical output voltage from the pulse generator. The pulse width was typically 40 ns, with a rise time of <10 ns. Voltage pulses up to 10 kV could be generated, although ultimately the experiments were limited by surface breakdown of the DUT.

Figure 1 shows that the DUT was placed in series with a 50 Ω current viewing/limiting resistor, also monitored by a Tektronix 7912. The resistance of the DUT was generally in the MΩ range, so essentially all the voltage from the pulser was dropped across the GaAs. Measured current was dominated by capacitive displacement at the beginning and end of the pulse. As a result, conduction current levels were not measurable, but given the resistivity of the material were probably in the mA range. The 50 Ω resistor was used to limit the current in the event of breakdown, and to maintain good high-frequency characteristics for subsequent experiments in which the DUT was switched with another Nd:YAG Laser.

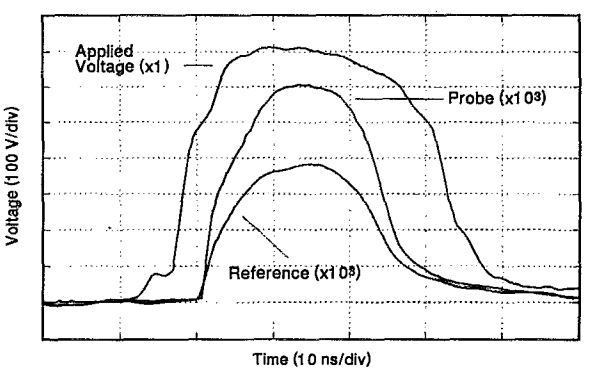

FIG. 3. Typical oscilloscope traces of the applied voltage pulse and the probe and reference photodiode response to the laser diode. The photodiode signals are scaled up by a factor of 10^3.

The DUT was probed optically with light from a temperature-controlled pulsed laser diode (Laser Diode Inc., LD-235), a 1 kW array driven by a commercial diode driver (Directed Energy Inc., LDX-P-100) which could produce an optical pulse width down to 20 ns. The laser was placed in a protective housing (nitrogen purged to prevent condensation problems) and the temperature was varied between 5 and 40 °C with a thermoelectric heat pump. This temperature range changed the center wavelength of the laser diode output from 902 to 911 nm, respectively, as measured with a 0.5 m McPherson spectrograph.

Light from the laser diode source was beam split with a microscope slide, with the reflected light sent to a reference photodiode to monitor shot-to-shot variations in the output intensity of the laser. The transmitted portion was focused with a lens, diffused, and directed onto the GaAs sample. An aperture behind the DUT ensured that only light actually transmitted through the sample was collected by another lens and detected with either a photodiode or a CCD camera. The photodiode signal was acquired with a second Tektronix 7912. The camera was a computer-controlled Electrim EDC-1000 which allowed digital acquisition of the image with a minimum shutter time of 200 ms.

Figure 3 also shows typical traces for the other reference and probe photodiode signals in the experiment. A Stanford Research Systems DG535 delay generator controlled the relative firing time of the voltage pulse and laser diode such that the 20 ns laser pulse occurred in the center of the 40 ns voltage pulse.

To account for possible temperature effects, we consider the worst case energy which could be deposited into the GaAs. The total capacitive energy stored in the transmission line pulser was a maximum of 8 mJ at 8 kV charging voltage (required to get about 40 kV/cm on the sample). Based on the imaging results reported below, we assume all this energy to be deposited uniformly into the GaAs. Given the volume of our sample (0.675×1.9×10 mm), the mass density of GaAs (5.32 g/cm^3) and the specific heat (0.35 J/g °C), then the maximum change in temperature due to the voltage pulse would be less than 0.4 °C. This is too small to significantly shift the absorption spectrum, so the Franz–Keldysh effect should be the only mechanism for absorption changes in our experiment.

IV. RESULTS

A. Spatially integrated photodiode measurements

Experimentally we observed the Franz–Keldysh effect as a decrease in the probe photodiode response as a function

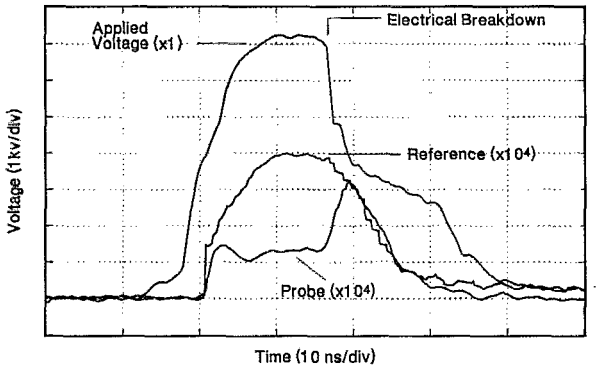

FIG. 4. Oscilloscope traces showing the applied voltage pulse and the electroabsorption effect on the probe photodiode signal when a breakdown occurred during the measurement. The reference signal was normalized to be the same as the zero-field probe signal. Photodiode traces are scaled by 10^4.

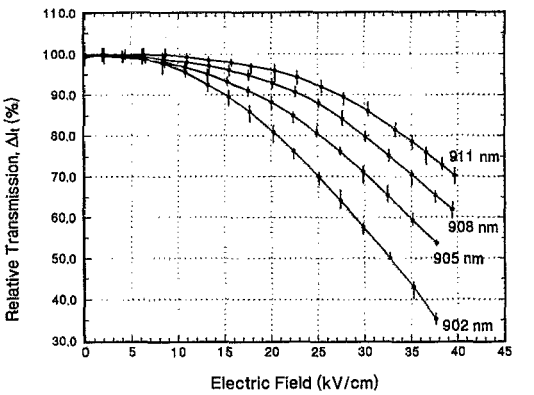

FIG. 5. Relative change in measured probe response compared to the zero-field value for 902, 905, 908, and 911 nm laser diode center wavelength. Lines are drawn through the average of ten consecutive measurements, with the error bars representing the extremes. Values were also normalized with respect to the reference photodiode signal to account for shot-to-shot variations in the laser diode intensity.

of the laser diode wavelength and the applied field. Figure 4 shows an applied voltage pulse and the associated reference and probe photodiode signals. The reference and probe signals are normalized such that with no applied field they have the same shape and amplitude. The laser diode fired at approximately the peak of the voltage pulse, and the probe response indicates the transmitted light is reduced to about one third of the zero-field level.

The traces in Fig. 4 were chosen because they also show the effect of a surface breakdown which occurred toward the end of the voltage pulse. The breakdown effectively shorts out the GaAs, evidenced by the drop in voltage to half the peak value. With a small field remaining across the DUT (<5 kV/cm) the absorption coefficient returns to almost the zero-field value and the probe signal increases to nearly the same level as the normalized reference signal. The transmission intensity increased at the same rate as the voltage decreased, indicating the Franz–Keldysh measurement has better than ns response time.

Figure 5 shows the relative change in the transmitted laser intensity as a function of electric field at the four measured laser wavelengths. Relative change was defined as

$$\Delta I_T(\lambda,E)=\frac{I_t(\lambda,E)}{I_t(\lambda,0)}, \tag{4}$$

where $I_t(\lambda,E)$ is the transmitted intensity with applied electric field E measured with the probe photodiode at wavelength λ.

The error bars in Fig. 5 are an indication of the wavelength instability of the laser diode. When the temperature dependence of the laser diode wavelength was checked with the spectrograph, some shot-to-shot shift in the peak of the output spectrum was observed. In our measurements this translates into variations of the transmitted intensity. The error bars represent the extremes for ten consecutive measurements, with the lines drawn through the average. These curves are also corrected for the shot-to-shot variation in the total output intensity of the laser diode, as monitored by the reference photodiode.

The results of Fig. 5 can be used to calculate the numerical shift in the absorption coefficient as a function of electric field and wavelength. The major assumption in this calculation is that the electric field was distributed uniformly across the GaAs during the voltage pulse (i.e., no significant voltage was dropped across the contacts and no high-field domains formed in the DUT). Since the applied voltages for these measurements were up to 8 kV, the first situation is unlikely, as contact potentials are typically on the order of volts. The imaging results presented below will show that the assumption of spatial uniformity is correct.

Taking multiple reflections into account (but ignoring interference effects) and given that our experiment measured the difference between two transmitted intensities, the value of the absorption coefficient was given by

$$\alpha(\lambda,E)=-\frac{\ln[z(\lambda,E)]}{x}, \tag{5}$$

where

$$z(\lambda,E)=\frac{-1}{2T(\lambda,E)}\left(\frac{1}{R}-1\right)^2+\sqrt{\left(\frac{1}{2T(\lambda,E)}\right)^2\left(\frac{1}{R}-1\right)^4+\frac{1}{R^2}} \tag{6}$$

and

$$T(\lambda,E)=\frac{1_t(\lambda,E)}{I_0}=\frac{I_t(\lambda,0)}{I_0}\Delta I_t(\lambda,0). \tag{7}$$

I_0 and I_t are the incident and transmitted light intensity, respectively, R is the dielectric reflection coefficient, x is the sample thickness, and α is the local electric field and wavelength-dependent absorption coefficient. R also has some electric field dependence because the dielectric constant is related to the absorption coefficient through the Kramers–Kronig relations, but the variation is negligible in our range of interest and was therefore ignored. This calculation also assumes that the electric field is uniform through the depth of the sample.

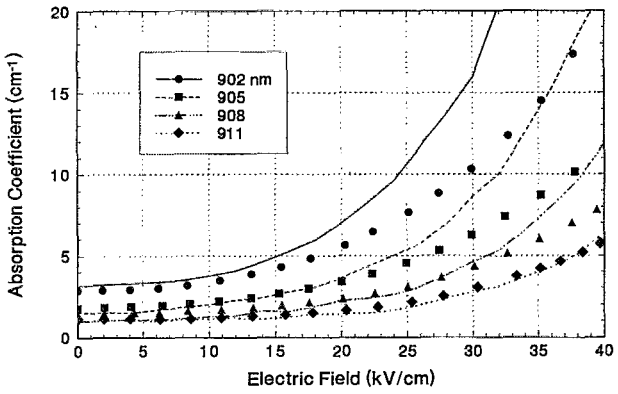

FIG. 6. Measured and calculated dependence of the absorption coefficient as a function of electric field and wavelength. Symbols represent values obtained from the average points in Fig. 5. Values represented by lines are calculated from Eq. (2) and the absorption spectrum shown in Fig. 7.

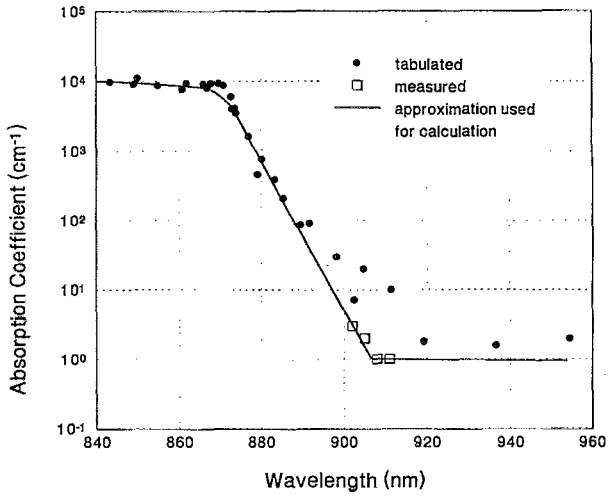

FIG. 7. Zero-field absorption spectrum used to calculate the electroabsorption shift. The solid circles represent tabulated values from Ref. 20, the empty squares are zero-field measurements with the laser diode, and the line is a piecewise approximation used to calculate the absorption shift in Fig. 6.

The ratio $I_t(\lambda,0)/I_0$ is a measure of the zero-field absorption and was experimentally determined simply by placing the photodiode directly behind the DUT to measure I_t, then removing the GaAs to measure I_0. These values are shown as the empty square points in Fig. 7. Taking $R=0.32$ for GaAs and $x=675$ μm for the sample thickness we calculated the absorption dependence using the averaged points in Fig. 5.

The plotted points in Fig. 6 show the measured variation in absorption coefficient as a function of wavelength and field. The values are generally consistent with the literature in terms of both the numbers and the dependence on the electric field.[11–13] At all wavelengths there is about a factor of 5 increase in α for a 40 kV/cm electric field. In an absolute sense, the 902 nm curve is shifted the most because that wavelength is closest to the band edge and is most strongly affected by the exponentially increasing character of the spectrum.

The solid lines in Fig. 6 show calculated values for the electroabsorption shift using Eq. (2). Figure 7 shows tabulated values[20] of zero-field absorption coefficient as well the experimentally determined numbers for our GaAs sample in the 902–911 nm range. The solid line drawn through the points is a piecewise approximation for the zero-field spectrum to simplify the numerical calculation.[21] We put emphasis on the tabulated values for the shorter wavelengths, since this region represents the fundamental GaAs character of the material (i.e., the band gap) and on our experimentally obtained values at the longer wavelengths. The absorption coefficient between these regions was assumed to vary exponentially.

The experimental results show good agreement with the calculated shift at long wavelengths. The deviation increases with decreasing wavelength. The largest difference is evident at 902 nm, where the measured change is smaller than what was calculated by almost a factor of 2 at 40 kV/cm. This indicates that the assumed long-wavelength character of the absorption between our measured values and those at the band edge is not correct.

B. Spatially resolved imaging

Figure 8 shows results of imaging experiments performed at a probe wavelength of 902 nm with the same GaAs sample using a CCD camera instead of the photodiode. The pictures show that the light intensity transmitted through the sample is relatively uniform at zero field. The gray level for zero field was adjusted either by varying the probe laser intensity, or by changing an aperture on the camera lens. The CCD camera had 256 gray levels (8 bit) with a value of 256 representing white and zero for black. The average transmitted light intensity at zero field was set at about 220 so that variations in the light source were not lost in the saturation of the camera.

The progression of images in Fig. 8 shows that the gray level of the images decreased in a spatially uniform manner as the electric field increased. For fields less than about 10 kV/cm there is little obvious change to the eye, but digital processing of the image does find some gray level shift (Fig. 9). At about 15 kV/cm the overall image intensity clearly decreased and continued to do so as the field increased.

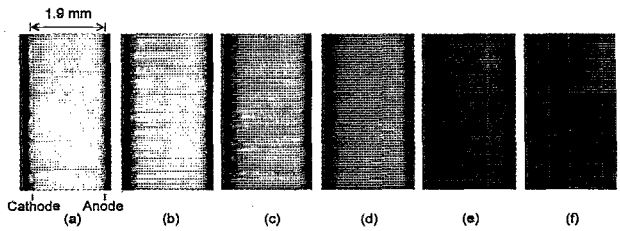

FIG. 8. Gray-scale pictures showing the change in transmission at 902 nm with electric field. An average gray level was found for each picture from a large rectangular region centered in each image and away from all edges. The field and corresponding gray levels were: (a) 0 kV/cm, 216; (b) 12.8 kV/cm, 198; (c) 20.1 kV/cm, 165; (d) 24.8 kV/cm, 131; (e) 32.7 kV/cm, 58; (f) 38.2 kV/cm, 0. The histogram spread of gray level around the average value for a given image was typically ±20.

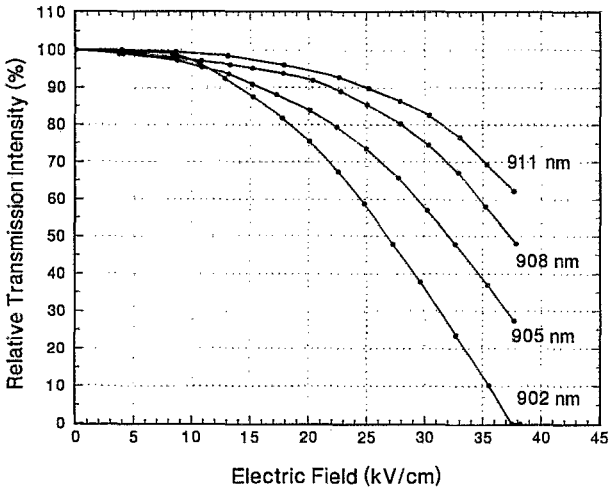

FIG. 9. Relative change in average image gray level compared to the zero-field value for the four laser diode wavelengths. Each point represents one image.

Above 37 kV/cm there was no longer any transmitted light detected by the CCD camera.

There is some structure (spatial intensity variation) in the images at higher fields, but closer examination showed that this same structure was present in the zero-field image. The structure is not as visible in the zero-field image because the contrast is too low. We conclude that the electroabsorption shift was uniform across the sample and the assumptions made in the integrated measurements are valid.

Similar sets of images were obtained at the other wavelengths we measured. These images were digitally processed and Fig. 9 shows the relative change in gray level for the four wavelengths. The value of the gray level for an image was defined as the peak of the histogram for an area of the image selected from the center. Relative change in gray level was then defined as for the intensity above.

As would be expected, the intensity change decreases with increasing wavelengths. A field of 40 kV/cm which caused a 100% change at 902 nm causes about 40% change at 911 nm. These results are also subject to the shot-to-shot variation seen in Fig. 5, but only one image was acquired for each field and wavelength value. This may explain the behavior at low fields, where it appears that the 902 nm curve stays above the 905 nm curve. This variation is within the error limits of the experiment.

C. Electric field diagnostics of photoconductive switches

The Franz–Keldysh method of electric field measurement was applied to the study of processes leading to breakdown phenomenon in high-voltage high-power GaAs photoconductive switches. At fields typically between 4 and 10 kV/cm, depending on the impurity type and concentration, a GaAs switch which is triggered into a conducting state by laser illumination returns to its initial high resistivity state when the photogenerated carriers recombine. Above this value the switch generally does not recover to a high resistance, but transfers into a persistently conductive mode

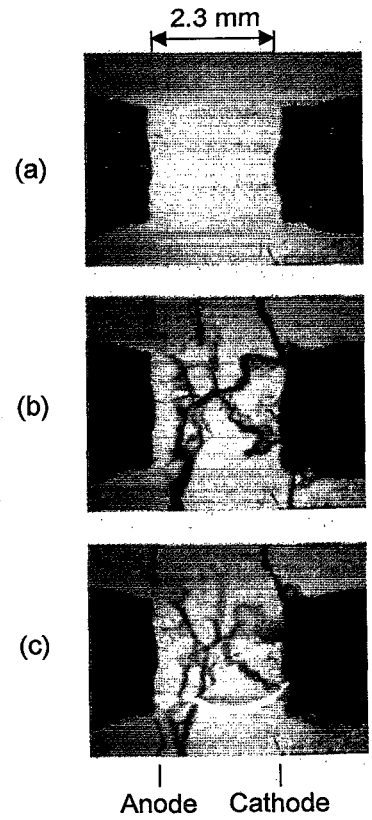

FIG. 10. Electroabsorption images using a 25 ns, 908 nm laser pulse to illuminate a GaAs photoconductive switch during a switching event. The totally black regions on the edges indicate the Au:Ge contacts, separated by 2.3 mm. (a) shows a typical transmission image with no applied field and no laser interaction. In (b) the switch was pulsed biased to 2.75 kV for 300 ns and turned on with a Nd:YAG laser (1 mJ/cm^2, 1064 nm, 7 ns pulse width). The electric field distribution was probed 20 ns after the turn on laser and no subsequent lock-on occurred. (c) shows the same conditions as (b) except that a lock-on filament formed after the electric field was probed. The filament is seen in the lower portion of the image as the white track connecting the contact regions.

(lock-on) in which the current flows in a filament.[22] Current only stops flowing when the energy source is depleted or the switch is damaged.

Lock-on is of interest from several perspectives. Breakdown can be a problem because it usually leads to damage and thus shorter switch lifetime. Understanding processes leading to breakdown could therefore lead to preventive measures which give longer device performance. From a different perspective, however, lock-on in GaAs switches can be attractive because it provides a "trigger" mechanism, where a little optical energy can be used to activate a switch into a permanent conductive state, similar to a laser triggered spark gap. Generally these switches are used in applications where lifetime is not of major importance. Understanding breakdown in this case could help increase the device performance.

The Franz–Keldysh field plotting technique was applied to study lock-on in GaAs. Results of these experiments will be published more completely elsewhere, but as a demonstration of the method transmission images at 908 nm of a switch during activation are shown in Fig. 10. Figure 10(a) shows a zero-field transmission image. The dark squares on

each side of the picture are Au:Ge contacts evaporated onto the surface of a semi-insulating GaAs wafer. 2.5 kV (10.8 kV/cm average field) was applied across the contacts for 300 ns and an Nd:YAG laser at 1064 nm (10 ns pulse width, 1 mJ/cm^2) was used during the voltage pulse to turn the switch on. Figure 10(b) shows that multiple regions or domains of high electric field form at the cathode contact and in the space between the contacts after the switch is activated by the laser. These domains were always present regardless of the applied field (although the character changed) whenever the switch was activated by the laser. Application of the voltage pulse alone caused no domain formation, and the average field was too low to observe uniform darkening as seen in the calibration measurements.

Figure 10(c) shows the same switch probed for the case when a lock-on mode developed, as evidenced by the white filament connecting the two electrodes (visible due to recombination emission). The open shutter character of the camera integrates the probe and breakdown events. The probe was fired before the filament developed and thus gives a snapshot of the electric field distribution leading to breakdown. The filament track was always normal to the direction of the electric field domains. This observation was consistent in other switches and may indicate that the breakdown starts in the high-field domain.

The calibration measurements described above give us some numerical measure of the field strengths required to modulate the transmitted light intensity. The high-field domains shown in Fig. 10 show complete extinction of the transmitted light intensity. From Fig. 9, a field of 40 kV/cm only reduces the light transmission by about 50% at 908 nm. Thus we can set a threshold value for the field in the domains of at least 40 kV/cm. Extrapolating the curve in Fig. 9 leads to a value of around 50 kV/cm.

V. DISCUSSION

A method for measuring the electric field in GaAs has been developed for use as a diagnostic tool to understand photoconductive switch breakdown. Calibration of the method was performed to measure the field induced change in absorption coefficient in semi-insulating GaAs in a wavelength range from 902 to 911 nm. At 902 nm it caused a factor of 5 change in the absorption coefficient for a field of 40 kV/cm. At longer wavelengths the magnitude of the shift was less pronounced, consistent with previously reported values. Spatial imaging of the absorption modulation (and thus the field distribution) was obtained using a CCD camera.

The calibration allows us to map and roughly quantify the field distribution in GaAs, or another material using GaAs as a proximate probe. Even with this relatively simple experimental arrangement, electric field differences on the order of 5 kV/cm could be resolved in the imaged experiments. A camera with more dynamic range and more stable probe light source would enable better field resolution. The spatial resolution of the measurement would ultimately be limited by the wavelength of the probe laser due to diffraction effects. Thus imaging on the order of 1 μm should be readily obtained. We have done some preliminary microscopy which demonstrated resolution of less than 5 μm.

Temporally a measurement with this method will ultimately be limited by the Heisenberg uncertainty relation for energy and time. As a rough estimate, if we require the uncertainty in the laser probe energy to be less than 10 meV (i.e., less than the probable effective Franz–Keldysh shift), then the time required for the measurement will be limited to $\Delta t > \hbar/\Delta E \approx 2.5$ ps. Experimental studies have demonstrated picosecond temporal resolution.[23]

These results also provide support for the concept of a commercial GaAs electric field probe.[24] GaAs coupled to the end of an optical fiber could be used to monitor the electric field in, for instance, electric utility equipment. The fiber optic connection would allow such a probe to be operated remotely and with complete electrical isolation to protect control electronics. With phase sensitive detection, such a device could resolve the electric field to within 1 kV/cm.

ACKNOWLEDGMENT

This work was supported by BMDO and managed through ONR. The Contract Manager was G. Roy.

[1] W. R. Donaldson, L. Kingsley, M. Weiner, A. Kim, and R. Zeto, J. Appl. Phys. **68**, 6453 (1990).
[2] K. H. Schoenbach, J. S. Kenney, F. E. Peterkin, and R. J. Allen, Appl. Phys. Lett. **63**, 2100 (1993).
[3] K. H. Schoenbach, J. S. Kenney, A. Koenic, B. J. Ocampo, R. F. K. Germer, and H. J. Schuls, Proceedings of the 8th IEEE Pulsed Power Conference, San Diego, CA, 1991, p. 105.
[4] R. A. Falk, J. C. Adams, and G. Bohnhoff-Hlavacek, Proceedings of the 8th IEEE Pulsed Power Conference, San Diego, CA, 1991, p. 237.
[5] R. A. Falk, J. C. Adams, S. G. Ferrier, and C. D. Capps, Proceedings of the 9th IEEE Pulsed Power Conference, Albuquerque, NM, 1993, p. 88.
[6] J. C. Adams, C. D. Capps, R. A. Falk, and S. G. Ferrier, Appl. Phys. Lett. **63**, 633 (1993).
[7] See any basic text on optical processes in semiconductors, e.g., J. I. Pankove, *Optical Processes in Semiconductors* (Dover, New York, 1971).
[8] P. S. Cho, J. Goldhar, and C. H. Lee, Proceedings of the 9th IEEE Pulsed Power Conference, Albuquerque, NM, 1993, p. 672.
[9] W. Franz, Z. Naturforsch. **13**, 484 (1958).
[10] L. V. Keldysh, Sov. Phys. JETP **7**, 788 (1958).
[11] G. E. Stillman, C. M. Wolfe, C. O. Bozler, and J. A. Rossi, Appl. Phys. Lett. **28**, 544 (1976).
[12] T. E. Van Eck, L. M. Walpita, W. S. C. Chang, and H. H. Wieder, Appl. Phys. Lett. **48**, 451 (1986).
[13] D. R. Wright, A. M. Keir, G. J. Pryce, J. C. H. Birbeck, J. M. Heaton, R. J. Norcross, and P. J. Wright, IEEE Proc. **135**, 39 (1988).
[14] W. Szuszkiewics, *Properties of Gallium Arsenide*, 2nd ed. (INSPEC, New York, 1990), p. 180.
[15] J. A. Lowrey, J. Appl. Phys. **66**, 4927 (1989).
[16] K. Seeger, *Semiconductor Physics* (Springer, New York, 1973).
[17] K. Tharmalingam, Phys. Rev. **130**, 2204 (1963).
[18] J. Callaway, Phys. Rev. **130**, 549 (1963); 134A, 998 (1964).
[19] H. D. Rees, J. Phys. Chem. Solids **29**, 143 (1968).
[20] D. E. Aspnes, *Properties of Gallium Arsenide*, 2nd ed. (INSPEC, New York, 1990), p. 147.
[21] I. Galbraith and B. Ryvkin, J. Appl. Phys. **74**, 4145 (1993).
[22] F. J. Zutavern, G. M. Loubriel, M. W. O'Malley, L. P. Shanwald, W. D. Helgeson, D. L. McLaughlin, and B. B. McKenzie, IEEE Trans. Electron Devices **ED-37**, 2472 (1990).
[23] C. V. Shank, R. L. Fork, B. I. Greene, F. K. Reinhart, and R. A. Logan, Appl. Phys. Lett. **38**, 104 (1981).
[24] M. S. Mazzola, K. H. Schoenbach and F. E. Peterkin, to be published in Proceedings of the 4th Biennial Industrial Electric Power Applications Symposium, New Orleans, Nov. 1994.